



Preparation of multifunctional gas-diffusion electrode and its application to the degrading of chlorinated phenols by electrochemical reducing and oxidizing processes

Hui Wang^{a,*}, Zhaoyong Bian^{b,**}, Guang Lu^a, Lei Pang^a, Zhipeng Zeng^a, Dezhi Sun^a

^a College of Environmental Science and Engineering, Beijing Forestry University, Beijing 100083, PR China

^b College of Water Sciences, Beijing Normal University, Beijing 100875, PR China

ARTICLE INFO

Article history:

Received 19 March 2012

Received in revised form 15 May 2012

Accepted 20 June 2012

Available online 27 June 2012

Keywords:

Chlorinated organic pollutants

Palladium-modified electrode

Reduction and oxidation processes

Reductive dechlorination

ABSTRACT

Multifunctional gas-diffusion electrode with electrochemical reduction and oxidation properties was achieved based on the palladium-modified activated carbon (Pd/C). Pd/C catalysts were prepared using the formaldehyde reduction from nitric acid treated activated carbon and fully characterized by Boehm titration method, X-ray diffraction (XRD), scanning electron microscopy (SEM), transmission electron microscopy (TEM), and cyclic voltammetry (CV) techniques. The electrochemical degradation of three typical chlorinated phenols (4-chlorophenol, 2,4-dichlorophenol and pentachlorophenol) was investigated in a diaphragm electrolysis system with the Pd/C gas-diffusion electrode as a cathode, feeding firstly with hydrogen gas and then with air. The electrolysis system with 15% mass fraction nitric acid pretreated activated carbon showed better electrocatalytic activity compared to those from other mass fractions nitric acid, due to the active organic function groups increased on the surface of the activated carbon. When the ratio of Pd/C was low, Pd particles with an average size of 3.5 nm were highly dispersed in the activated carbon with an amorphous structure. The Pd/C gas-diffusion cathode cannot only reductively dechlorinate chlorinated phenols by feeding hydrogen gas, but also accelerate the two-electron reduction of O₂ to H₂O₂ by feeding air. Therefore, the removal efficiency of chlorinated phenols reached almost 100%, conforming to the sequence of 4-chlorophenol, 2,4-dichlorophenol and pentachlorophenol. The dechlorination of three chlorinated phenols exceeded 80% after 100 min. For H₂O₂ and HO[•] existed in the catholyte, the mineralization of organic pollutants in the cathodic compartment was better than that in the anodic compartment. Finally, chlorinated organic pollutants were efficiently degraded by the combined processes of reduction and oxidation in the present system.

© 2012 Elsevier B.V. All rights reserved.

1. Introduction

Among the various organic wastes, chlorinated phenols are harmful environmental pollutants due to their high toxicity, recalcitrance, bioaccumulation, and persistence in the environment [1,2]. The resistance to degradation as well as the toxicity of chlorinated phenols increases with the number of chlorine substituents [3]. As the accumulation of chlorinated phenols in the environment has become a serious problem nowadays, it is very urgent to develop an effective method to remove these contaminants.

Traditional treatment processes such as biological treatments are not very effective for degradation of chlorinated phenols. However, advanced oxidation processes (AOPs) can be used to

effectively treat wastewater containing chlorinated phenols [4–6]. The electrochemical oxidation for the treatment of wastewater containing chlorinated phenols has attracted much attention recently, because of its ease of control, amenability to automation, high efficiency, and environmental compatibility [7]. At present, dimensionally stable anodes (DSA) have been used for the oxidation of chlorophenol pollutants [8]. Usually, the electrochemical treatment can actualize the mineralization of organic pollutants by the stronger oxidant such as hydroxyl radicals (HO[•]), which are in situ generated by the electrochemical reaction on the electrode surface [9]. Very recently, indirect electro-oxidation methods for the wastewater treatment involving the H₂O₂ electrogeneration have been developed. Additionally, carbons materials such as carbon/polytetrafluoroethylene (C/PTFE) [10–14], carbon nanotubes [15], graphite [16–18], carbon felt [19–21] and reticulated vitreous carbon [22,23] are classified as electrode materials for the electrochemical production of H₂O₂. However, advanced oxidation processes including electrochemical oxidation usually open

* Corresponding author. Tel.: +86 10 62336615; fax: +86 10 62336596.

** Corresponding author. Tel.: +86 10 59893263; fax: +86 10 59893263.

E-mail addresses: wanghui@bjfu.edu.cn (H. Wang), bian@bnu.edu.cn (Z. Bian).

Table 1

Experimental conditions of the preparation procedure, Pd loading and mean Pd particle sized for several catalyst samples.

Catalyst(sample)	T(°C)	C _{HNO₃} (%)	Pd loading(wt.%)	Pd particle size (nm) measured by	
				XRD	TEM
a	–	–	0	–	–
b	100	15	0.5	6.0	5.7 ± 0.5
c	80	15	0.5	3.5	3.3 ± 0.8
d	80	15	1	4.9	4.8 ± 0.7
e	80	15	3	6.4	6.1 ± 0.8
f	80	15	5	8.3	8.0 ± 0.6
g	80	20	5	9.8	9.5 ± 0.8
h	80	8	5	9.6	9.3 ± 0.7
i	80	15	10	12.1	11.8 ± 0.8

aromatic nucleus of chlorinated organic pollutants and then form many chlorinated aliphatic intermediates [24]. The accumulation of chlorinated intermediates may be even more toxic than their parent compounds.

It is well known that chlorinated compounds are toxic due to the chlorine contained in their structures. The possibility to gain exhaustive dechlorination of chlorinated aromatic compounds by an electrochemical reductive approach was disclosed in the 1970s. This method ensured the selective removal of chlorine atoms from various chlorinated aromatic compounds under mild experimental conditions. According to the literature [25,26], hydrogenolysis of the C–Cl bond is catalytically processed by the reaction of adsorbed organic substrate with the chemisorbed hydrogen. Then, the products desorbed from the surface of electrodes. However, most electrochemical reductive studies focus on the removal of chlorine atoms from the aromatic structure without further processes being applied simultaneously to treat the organic intermediates. Therefore, an effective and friendly method has been developed to treat contaminants of chloride compounds by using a combination process of electrochemical reduction and oxidation. In the cathodic compartment, the chlorine atoms of chlorinated phenols are removed from the aromatic structure and chlorinated phenols are reduced to non-chloride intermediates. Then, the non-chloride intermediates are oxidized and degraded in the anodic and cathodic compartments [27].

Activated carbon (AC) has a high surface area, bulk porosity and various surface chemical properties. It has been recognized as good adsorbent or support [28,29], especially hydrogenation and hydrodechlorination with palladium and platinum as active phase. Carbon-based catalysts offer significant advantages versus the conventional catalysts. For instance, there are various low price carbonaceous sources [30]. The adsorption capacity of AC is known to be a function of surface area, pore volume and porous structure. However, as a reducing agent, the surface chemical nature of AC plays an important role in the activity of carbon-based catalyst. And the surface chemistry of AC can be changed by the interaction between the carbon surface and the reactants adsorbed, such as the treatment with oxidants (O₂, HNO₃, H₂O₂, KMnO₄, HClO₄ and so on) [31–33]. HNO₃ treatment can affect the surface chemistry of AC moderately and produce appropriate amount of the oxygen-containing complexes and surface acid groups.

In this paper, the catalytic reduction and oxidation of chlorinated phenols by multifunctional Pd/C gas-diffusion electrode had been investigated. Firstly, Pd/C catalyst used for the gas-diffusion electrode was prepared and characterized by X-ray diffraction (XRD), scanning electron microscopy (SEM), transmission electron microscopy (TEM), and cyclic voltammetry (CV). Then, the degradation of three kinds of chlorinated phenols in a diaphragm cell was performed, with an organic synthesized diaphragm, a Ti/IrO₂/RuO₂ anode, and a self-made Pd/C gas-diffusion cathode. Finally, an effective and friendly method was developed to degrade chlorinated

compounds by using a combined process of reduction and oxidation.

2. Experimental

2.1. Preparation and characterization of Pd/C catalyst

Pd/C catalyst was prepared by the formaldehyde reduction of palladium salt on the activated carbon support. Nitric acid treatment was carried out by heating an appropriate amount of activated carbon in a nitric acid solution (8%, 15%, and 20%) at reflux temperature for 2 h. After that, the sample was washed with distilled water until neutrality and then dried overnight at 100 °C. Palladium chloride was firstly dissolved in a concentrated hydrochloric acid solution and then diluted with 15 mL of water. The solution of PdCl₂ was dropped into a vigorously stirred activated carbon solution at 80 °C (or 100 °C). The mixture was kept at 80 °C (or 100 °C) for 2 h and then was cooled to 40 °C. A 36% formaldehyde solution was added to the vigorously stirred mixture. After the addition, stirring was kept for 30 min, a 30% NaOH solution was then added dropwise to keep the mixture pH at 8–9. The formed catalyst was then washed six times by decanting with water to remove chloride until no chloride anion in the filtrate was detected with AgNO₃ solution. After being filtered on a sintered crucible, washed and dried, Pd/C catalysts with a different Pd load (0.1, 0.3, 0.5, 1, 3, 5, and 10 wt.%) were obtained and stored in a desiccator. Experimental conditions of the preparation procedure, Pd loading and mean Pd particle sized for several catalyst samples are summarized in Table 1.

The concentration distributions of oxygen functional groups on the surface of the activated carbon were obtained by Boehm titration [34]. The XRD patterns were used to identify every present phases and their crystallite sizes. The Pd/C catalyst was characterized by XRD with an X' Pert PRO MPD X-ray power diffractometer using Cu Kα radiation with a Ni filter. S-4800 SEM was used to study the surface morphology. In addition, the Pd particle morphology and size distributions were determined by JEM-2010F TEM microscope operated at an accelerating voltage of 200 kV.

2.2. Electrochemistry measurements

Electrochemical measurements (cyclic voltammogram, CV and differential pulse voltammogram, DPV) were recorded using a potentiostat/galvanostat (EG&G Model 273A) with a standard three-compartment cell consisting of a Pt wire as a counter electrode, an Ag/AgCl electrode as a reference, and the Pd/C catalyst (or activated carbon) modified electrode as a working electrode. The Pd/C catalyst (or activated carbon) modified electrodes were prepared according the following procedure: five milligram of Pd/C catalyst (or activated carbon) was suspended in a mixture of 1 mL of ethanol and 50 μL of Nafion® solution (5 wt.% Aldrich solution) to

prepare a catalyst ink. Then 10 μL of ink was transferred with an injector to the surface of a clean glassy carbon disk electrode (with area of 0.126 cm^2). After the ethanol evaporated, the electrode was heated at 75 $^\circ\text{C}$ for 10 min. 0.5 mol L^{-1} of Na_2SO_4 solution was used as an electrolyte, which was saturated with oxygen by feeding oxygen gas throughout the electrolysis. During the experiment process, the electrolyte temperature was kept constant at 25 $^\circ\text{C}$. The scan rate was 50 mV s^{-1} . Substrates were 2-chlorophenol (2-CP), 3-chlorophenol (3-CP), 4-chlorophenol (4-CP), 2,4-dichlorophenol (2,4-DCP), and 2,4,5-trichlorophenol (2,4,5-TCP).

2.3. Catalytic dechlorination and oxidation of chlorinated phenols

The Pd/C gas-diffusion cathodes were prepared according to the reported procedure [35]. Electrolysis was conducted in a terylene diaphragm cell of 100 mL with a Ti/IrO₂/RuO₂ anode (16 cm^2) and a gas-diffusion cathode (16 cm^2). A schematic diagram of the experimental setup has been described elsewhere [35]. A laboratory direct current power supply with current–voltage monitor was employed to provide the electric power. The experimental conditions were as follows: the initial chlorinated phenols (4-CP, 2,4-DCP, and PCP) concentration was 100 mg L^{-1} ; the current density was 39 mA cm^{-2} ; the concentration of supporting electrolyte (Na_2SO_4) was 0.1 mol L^{-1} ; the distance between electrodes was 2 cm; the initial pH was 7.0. Before starting electrolysis, hydrogen gas was fed for 5 min with the rate of 25 mL s^{-1} to keep dissolved gas saturation. Hydrogen gas was then fed into the gas compartment during 0–60 min (electrolysis time), following air.

The determination of chlorinated phenols in electrolyzed solutions were carried out using high-performance liquid chromatogram (HPLC, Shimadzu, Japan) analyses by comparing the retention time with those of the standard compounds. Samples of 20 μL filtered with PTFE filters of 0.45 μm were injected to the HPLC. The separation was performed using a Zentris ODS-SP C18 column (250 mm \times 4.6 mm, 5 μm) at a flow rate of 1.0 mL min^{-1} and at column temperature of 25 $^\circ\text{C}$. The mobile phase was methanol/water (v/v) at 80/20, and an UV detector was set at a wavelength of 280 nm. The total organic carbon (TOC) was detected by an Elementar High TOC analyzer. The concentration of chloride ion in electrolyzed solutions were determined using an ion chromatograph (ICS-3000, Dionex, America) by comparing the retention time of the standard compounds. Samples of 30 μL previously filtered with PTFE filters of 0.45 μm were injected to IC. The separation was performed using an AS-11 column at the flow rate of 1.2 mL min^{-1} . The column temperature was 30 $^\circ\text{C}$. The mobile phase were constructed by 5% (vol.) 5 mmol L^{-1} NaOH and 95% (vol.) deionized water in the 0–6 min, the volume of NaOH raised to 12% in the 6–41 min, the volume of NaOH reduced to 5% in the 41–42 min and remained 5% in the 42–50 min.

3. Results and discussion

3.1. Preparation and characterization of Pd/C catalyst

The importance of the surface properties of carbon substrates used as supports in heterogeneous catalysts has been clearly recognized. Strong acid oxidation plays a important role in the surface modification of carbon substrates. Nitric acid in various mass fractions (8%, 15%, and 20%) was used on activated carbon pretreatment. The nitric acid pretreated activated carbon samples were analyzed and compared with the original one. The amounts of oxygen functional groups (acidic, phenolic hydroxyl, carboxylic, and carbonyl groups) on the surface of the activated carbon by the nitric acid pretreated are showed in Fig. 1.

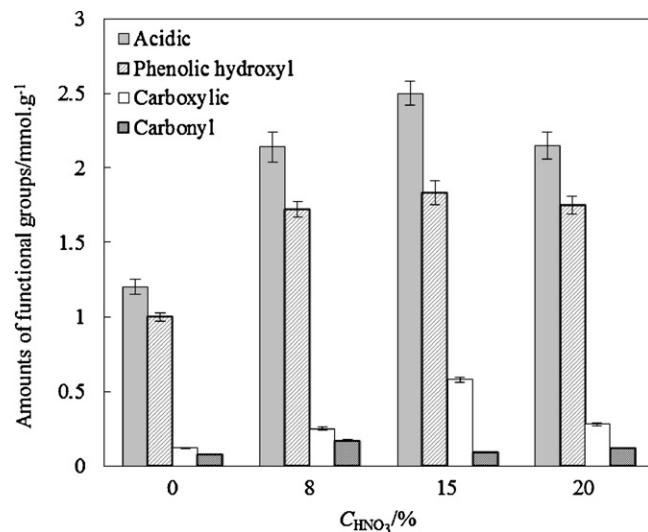


Fig. 1. Amounts of oxygen functional groups on the surface of the activated carbon by the nitric acid pretreated.

As shown in Fig. 1, the amount of acidic, phenolic hydroxyl, and carboxylic groups increased with the concentration of treated nitric acid until they reached the maximum. When 15% nitric acid was used as the oxidant, the maximum amount of acidic, phenolic hydroxyl, and carboxylic groups were 2.50 mmol g^{-1} , 1.83 mmol g^{-1} , and 0.58 mmol g^{-1} , respectively. Additionally, the acidic groups were the main content of the containing oxygen functional groups on the surface of pretreated activated carbon samples. The decrease of the amount of carbonyl groups was the result of the over oxidation in the nitric acid pretreatment. The complex chemistry of acidic surface functions has been reviewed [36]. In general, it is agreed that the most important surface groups in order of decreasing acidity are: carboxylic groups; phenolic hydroxyl; and carbonyl groups. That is to say, the activity of activated carbon for loading palladium species can be improved by increasing the content of the acidic containing oxygen groups on activated carbon. The degree of oxidation effect increased with the concentration of nitric acid for the pretreatment, because of the strongly oxidation reaction between drawback sites in activated carbon and the oxidant, nitric acid. The surface area and pore volume increased due to the collapse of the partly pore walls. In particular, the volume of the larger and middle micropores increased remarkably. When the concentration of nitric acid was 20%, strong over-oxidation induced a decrease in the micropore volume and subsequently in the mesopore volume, due to the serious collapse of the pores and block in the pores. Therefore, the 15% nitric acid was chosen as the best pretreatment oxidant.

XRD characterization of these samples was carried out to determine the crystal structures and the results are shown in Table 1 and Fig. 2.

As shown in Fig. 2, there are two broad diffraction peaks of activated carbon structure. The peaks at $2\theta = 40.08^\circ$, 46.78° , 68.26° , 82.20° were the diffraction peaks of Pd. There was no diffraction signal from other metals other than Pd in these samples. The samples b–d showed diffraction peaks of Pd with low intensity, due to the low Pd loading amount. Among samples e–i, obvious diffraction peaks of Pd could be observed with increasing of Pd loading amount. This suggested that Pd located on AC-HNO₃ is highly dispersed. The high dispersion could be attributed to the complex interaction of the metal precursor with oxygen containing functional groups in the surface of carbon supports. Zhu et al. [37] also reported that acid treatments of carbons may improve nickel distributions on the carbon support by making more nickel ions diffused into the inner

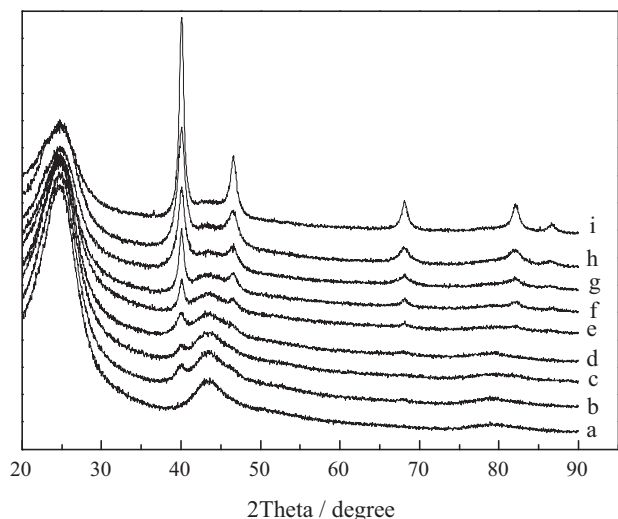


Fig. 2. X-ray diffraction patterns of Pd/C catalysts by the different experimental conditions.

pores of carbons. Hence an increase of the surface oxygen groups on AC-HNO₃ favored the dispersion of Pd on activated carbon, and treatments of activated carbon with HNO₃ made more palladium ions diffused into the inner pores of activated carbon.

The corresponding XRD patterns of Pd/C catalysts sample with a Pd load (0.1, and 0.3 wt.%) resembled only the features of the carbon support, which was consistent with SEM results. The size of Pd nanoparticles in these two samples was too small and the amount was low, which made it difficult to be detected. Pd/C catalysts with a Pd load 5 and 10 wt.% represented similar diffraction features to polycrystalline Pd of face centered cubic crystal (fcc) structure. The

only difference between XRD pattern of Pd/C-f and Pd/C-i sample was the diffraction intensity of Pd characteristic peaks when the carbon support was considered as reference. When the amount of loaded palladium increased in the Pd/C catalysts, tiny nanoparticles could agglomerate into bigger ones. And the width of the corresponding diffraction peaks of Pd/C-f was much broader, indicating the presence of much smaller size of Pd nanoparticles. Based on X-ray line broad method, the mean particle size of Pd/C-f was 8.3 nm, which is much smaller than 12.1 nm of Pd/C-i sample.

As shown in Table 1 and Fig. 2, when the temperature was 80 °C, the mean particle size of b–c samples was 3.5 nm. When the temperature was increased to 100 °C, the mean particle size was to 6.0 nm and the dispersion of Pd nanoparticles was deteriorated to some extent due to higher temperature treatment. This also indicated that treatment temperature had a important effect on the dispersion state of metal nanoparticles for the supported catalyst. With the temperature increasing, the binding strength of Pd particles on the surface of activated carbon decreased. Then the Pd nanoparticles favored agglomeration to increase the particle size and lead bad nanoparticles dispersion.

In order to estimate the geometry and the particle size of the Pd species, SEM and TEM image of Pd/C catalyst and the metal particle size distribution were measured (see Figs. 3 and 4). SEM and TEM image indicated that the dispersion of Pd nanoparticles on the carbon support was uniform and in a narrow particle size range.

Fig. 3 shows the SEM images of Pd/C-c and Pd/C-g samples obtained by the formaldehyde reduction method. It was clearly found that there were heavy agglomerations of Pd nanoparticles in Pd/C-g sample; while for Pd/C-c catalyst, highly dispersed Pd nanoparticles with an average diameter of 3.5 nm were uniformly supported on the carbon surface. This indicated that nitric acid pretreatment exhibited large advantages in the preparation of highly dispersed Pd nanoparticles. However, during the catalyst

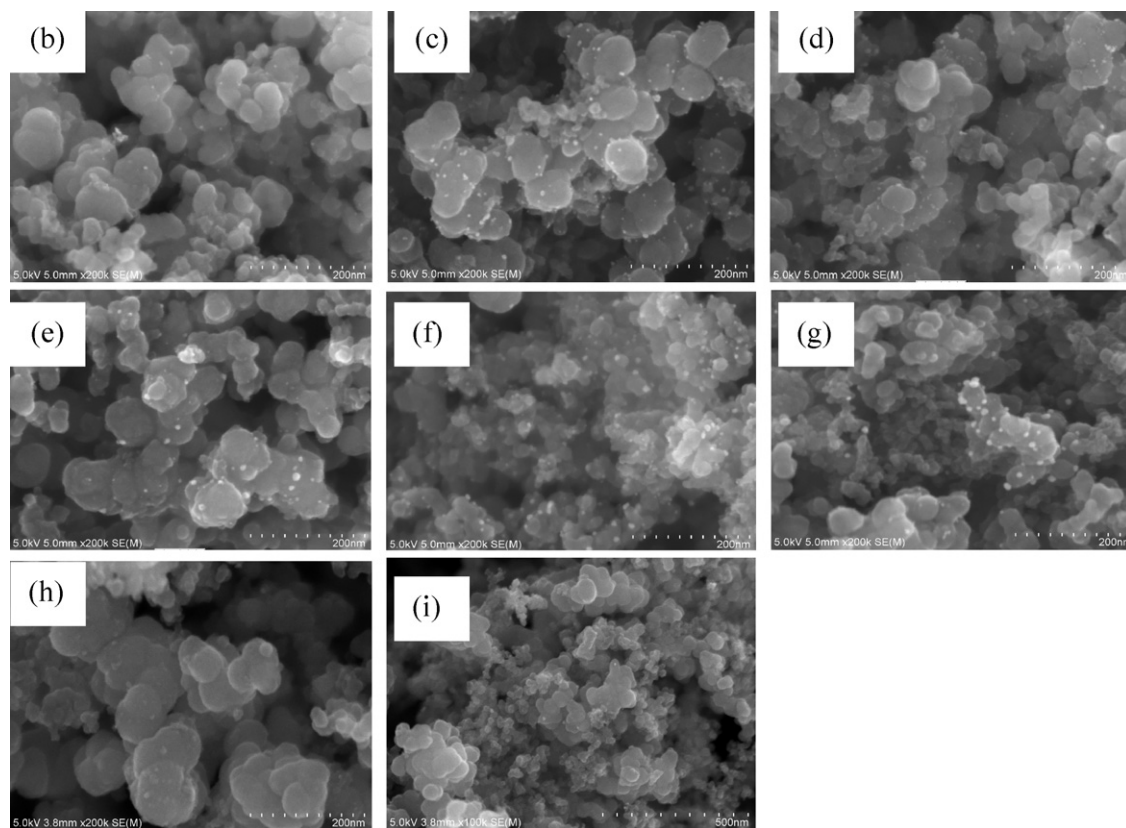


Fig. 3. SEM patterns of Pd/C catalysts by the different experimental conditions.

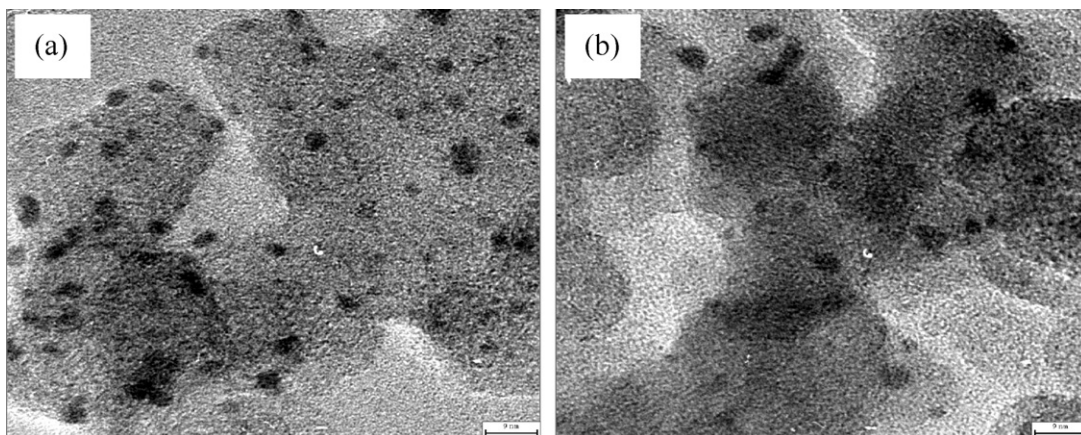


Fig. 4. TEM patterns of Pd/C-c (a) and Pd/C-d (b) catalyst samples.

preparation, Pd nanoparticles tend to agglomeration, because Pd is one of the strongest hydrolysable metals. As shown in Fig. 3b, when more palladium chloride was used during Pd catalyst preparation, the serious agglomeration of Pd nanoparticles happened. To obtain Pd/C catalyst with a good Pd nanoparticles dispersion, a Pd load 0.5 wt.% had been introduced during catalyst preparation.

TEM image of the as-received Pd/C-c is shown in Fig. 4a. No serious agglomeration of Pd nanoparticles on carbon support could be found in Pd/C-c sample. However, it should be noted that the TEM image of Pd/C-d mostly resembles the characteristic of activated carbon support (shown in Fig. 4b), with only a few tiny metal nanoparticles observed on carbon support. It could be found that large quantities of Pd nanoparticles were emerged on the carbon support with uniform distribution. The mean diameter of Pd/C-c was about 3.3 nm, which was analogous to that of Pd/C-d.

Therefore, the Pd/C catalyst (15% nitric acid pretreatment, mixture temperature 80 °C, Pd load 0.5 wt.%) was used for the electrocatalytic degradation of chlorinated phenols.

3.2. Electrochemistry test

Cyclic voltammetry method was employed to characterize the electrochemistry property of the prepared Pd/C catalyst. Fig. 5 shows CV and DPV curves in a 0.5 mol L⁻¹ Na₂SO₄ solution (pH 12.8 adjusted with NaOH solution) of the different catalyst electrode surfaces at precense of oxygen. There was a high reduction peak at about -0.20 to -0.40 V in the presence of oxygen in a basic solution. According to redox potential, the two-electron reduction of O₂ to peroxide anion (HO₂⁻) led the formation of reduction current peaks of prepared Pd/C catalyst in a basic solution. The reduction current peak of the Pd/C catalyst modified electrode was higher than that of the no catalyst modified electrode. The results indicated that Pd catalysts could promote the formation of H₂O₂. Additionally, the peak potential moved towards positive attributed Pd/C catalyst could reduce the applied voltage.

Cyclic voltammetry for 1 mmol L⁻¹ 2,4-DCP at a Pd/C catalyst showed the intensity of the oxidation peak increased and potential shifted negatively with increased sweep rate (ν), typical of an irreversible reaction (shown in Fig. 6). The dependence of the peak current i_p on $\nu^{1/2}$ showed that oxidation was diffusion controlled at this concentration (inset in Fig. 6).

Peak currents in the DPV of highly chlorinated phenols (1 mmol L⁻¹, scan rate 50 mV s⁻¹) shifted to less negative potentials (shown in Fig. 7), opposite to what might intuitively be expected, because highly chlorinated compounds were generally stronger resistant to oxidation. The chosen chlorinated phenols started to oxidize at the cathode potentials of -0.4 V, but

the current fall earlier in the voltammetric scan for the more highly chlorinated phenol congeners, which form more insoluble deposits. Fig. 8 shows that the onset of oxidation shifted to positive potentials at high pH. This indicated that the phenolate was oxidized more easily than the neutral phenol [38].

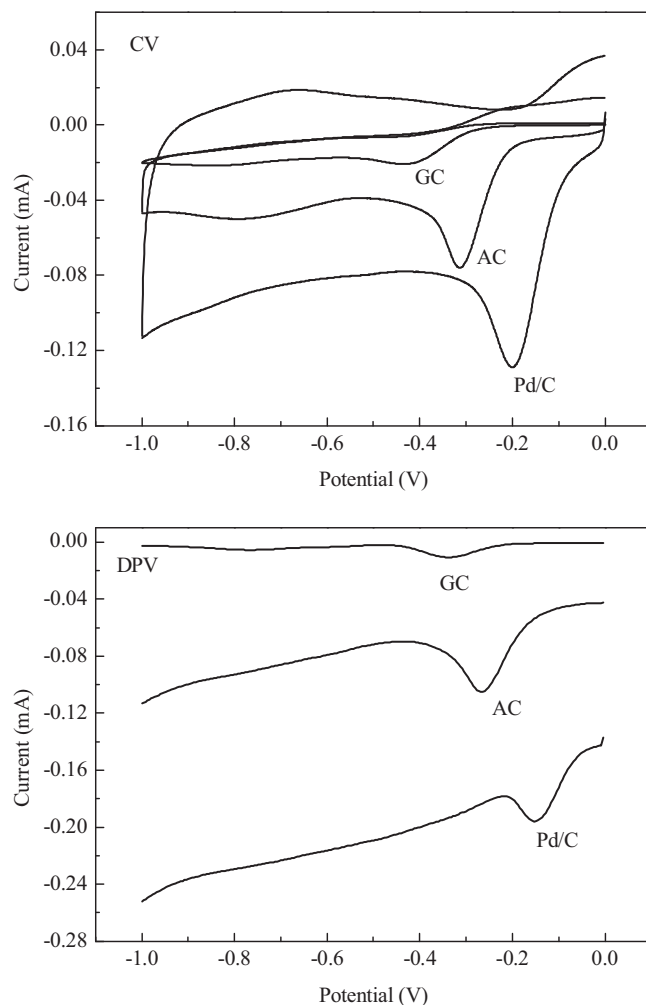


Fig. 5. CV and DPV curves at different catalysts in 0.5 mol L⁻¹ Na₂SO₄ solution (pH 12.8, feeding O₂).

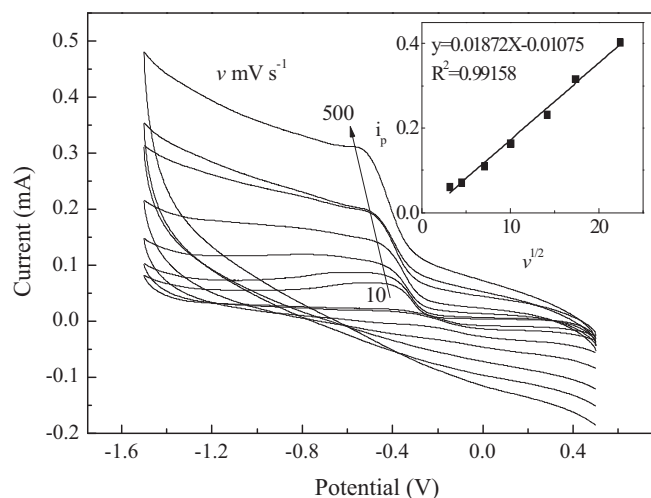


Fig. 6. Cyclic voltammograms (Pd/C catalyst, pH 12.8, feeding O_2) for the oxidation of 1 mmol L^{-1} 2,4-dichlorophenol at scan rates $10\text{--}500 \text{ mV s}^{-1}$.

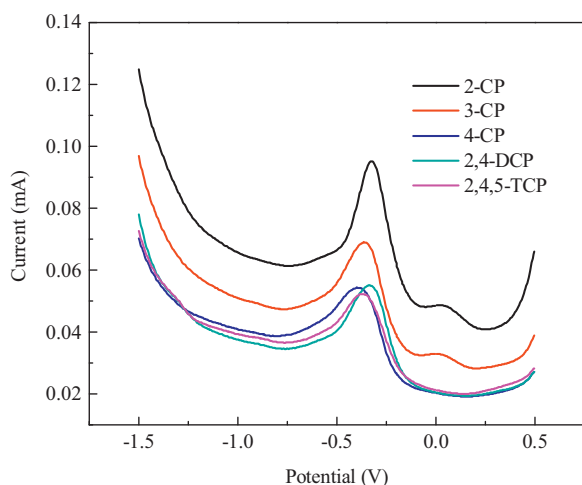


Fig. 7. DPV (Pd/C catalyst, pH 12.8, feeding O_2) for the oxidation of several chlorinated phenols (1 mmol L^{-1}).

3.3. Catalytic dechlorination and oxidation of chlorinated phenols

Fig. 9 shows the removal efficiency of chlorinated phenols and TOC removal with electrolysis time in the cathodic and anodic

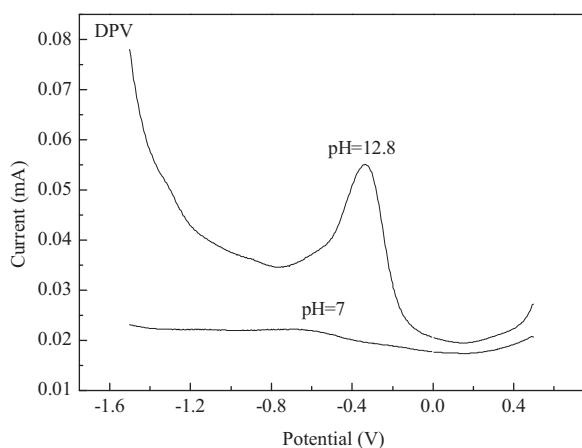


Fig. 8. DPV (Pd/C catalyst, feeding O_2) for the oxidation of 1 mmol L^{-1} 2,4-dichlorophenol at different pH.

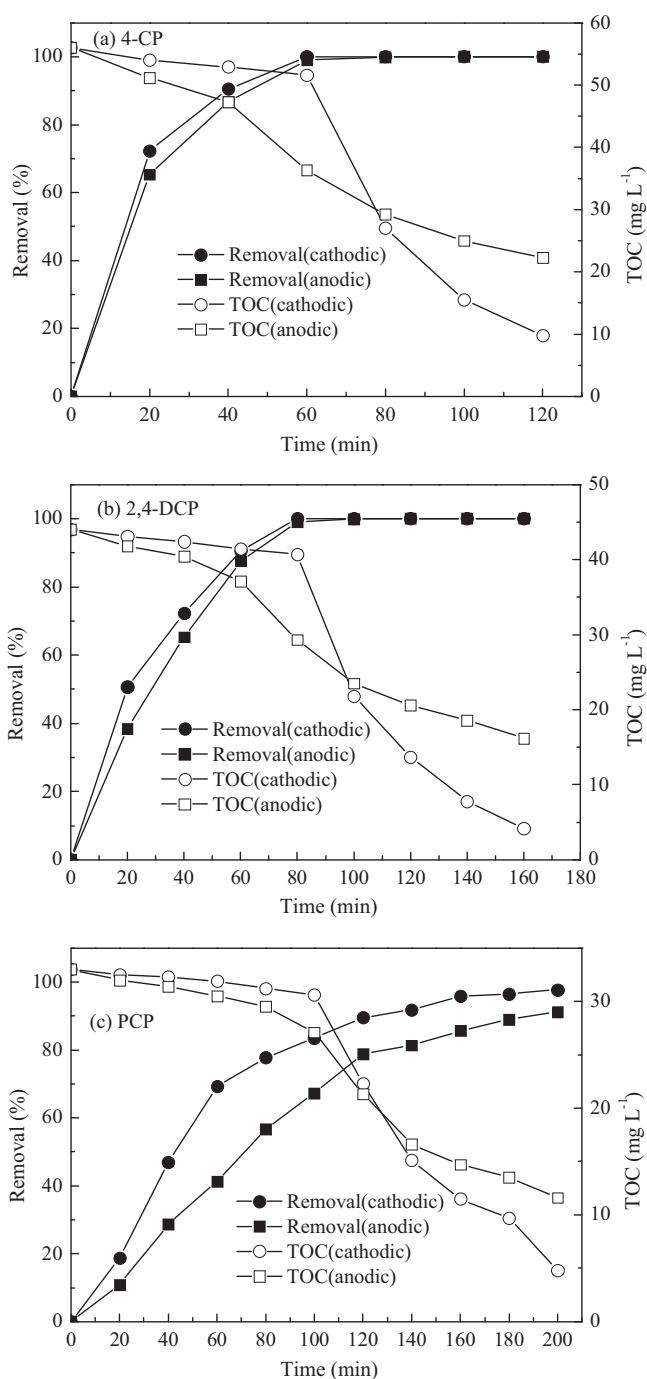


Fig. 9. Removal of chlorinated phenols and variation of TOC in the cathodic and anodic compartments with electrolysis time at feeding hydrogen and air by the Pd/C gas-diffusion electrode system.

compartments by the Pd/C gas-diffusion electrode system. In the initial 60 min, the removal efficiency of three chlorinated phenols remarkably increased with electrolysis time in the cathodic compartment by feeding hydrogen gas. The removal efficiency of 4-CP and 2,4-DCP reached about 100% at 60 and 80 min, respectively. This trend was attributed to the fact that in situ formed hydrogen atom was a powerful reducing agent that reductively dechlorinates chlorinated phenols, and reaction under hydrogen atmosphere was in favor of improving the removal efficiency of chlorinated phenols.

During the electrolysis process, the total TOC removal was lower than the corresponding degradation fraction of the target chlorinated phenols. It indicated that chlorinated organic pollutants were

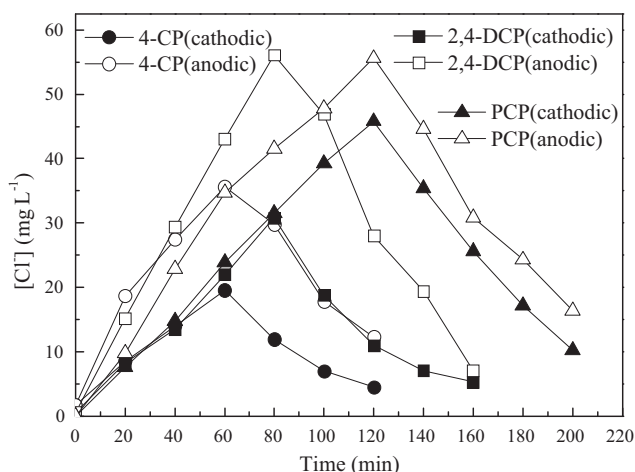


Fig. 10. Variation of Cl^- concentration in the cathodic and anodic compartments with electrolysis time.

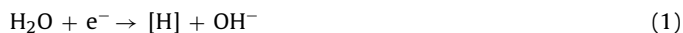
oxidized to smaller molecule intermediates. The removal efficiency for chlorinated organic compounds reached about 100%, conforming to the sequence of 4-CP, 2,4-DCP and PCP. The organics became more difficult to be oxidized with the increase of the number of chlorine atoms in the aromatic ring.

The concentration of chloride ion released from the target chlorinated organic compounds during the electrochemical oxidation was measured to evaluate the dechlorination process. The chlorine substituent in the organic compounds contributed to the toxicity of aromatic compounds. Therefore, the degree of dechlorination indirectly represented the detoxification degree. During the degradation process of 4-CP, 2,4-DCP and PCP, the changes of the concentration of chloride ion with electrolysis time in the cathodic and anodic compartments were illustrated in Fig. 10.

The initial solutions of chlorinated phenols had the dissociative chloride ion. The chloride ion concentration of 4-CP, 2,4-DCP and PCP increased in the both anodic and cathodic compartments with an increasing of electrolysis time during 0–60 min, 0–80 min electrolysis and 0–100 min, respectively. However, the concentration of chloride ion in the anodic compartment was higher than that in the cathodic compartment. This attributed to the fact that in the initial period of the experiment, the chloride ions of the cathodic compartment could diffuse to the anodic compartment through terylene diaphragm, due to the electro-static repulsion from the negatively charged cathode. For 4-CP, the concentration of chloride ion reached maximum after 60 min, and the degree of dechlorination reached about 95.3%. After 80 and 100 min, the concentration of chloride ion for 2,4-DCP and PCP reached the highest, and the degree of dechlorination reached about 92.4% and 82.3%, respectively. With the increase of electrolysis time, the concentration of chloride ion decreased in two compartments. It indicated that chloride ion was already oxidized to Cl_2 at the anode, as reported for the electrolysis of chlorophenol with BDD anode [39], and Cl_2 was immediately driven away from the reaction system [40]. The dechlorination effect of chlorinated phenols showed that 4-CP > 2,4-DCP > PCP. This can be attributed to that 2,4-DCP and PCP possessed one more chlorine atom than 4-CP in the aromatic ring, and the dechlorination difficulty of organics increased with the increase of the number of chlorine atoms in the aromatic ring.

Pd/C gas diffusion electrode played an important role in the dechlorination of chlorophenol contaminants due to its reduction activity. Palladium is not only a catalyst for the hydrogen atom formation but also a facilitator for the reductive dechlorination of chlorinated organic pollutants. In the cathodic compartment, the mechanism of the electrocatalytic destruction of carbon-chlorine

bond (R-Cl molecule) was described by the following equations. First, chemisorbed hydrogen atom ($[\text{H}]$) was formed on the cathodes surface by reduction of water [41,42].



At the same time, hydrogen gas was adsorbed on the surface of Pd and formed a powerful reducing species, $[\text{H}]$. Then, hydrogenolysis of the C–Cl bond of the absorbed chlorinated organic compounds proceeded in the presence of reducing species, $[\text{H}]$.



As shown in Fig. 9, in the initial 60 min, TOC removal in the cathodic compartment increased slightly with prolonged the electrolysis time in two systems. After 60 min, feeding air was used instead of feeding hydrogen gas, and TOC removal of the cathodic compartment markedly increased. Pd/C gas diffusion electrode played another important role in the degradation of chlorophenol contaminations due to its oxidation activity. Pd/C gas-diffusion electrode catalyzed the two-electron reduction of O_2 to H_2O_2 and HO_2^- , and then H_2O_2 and HO_2^- may be converted to HO^\bullet and $\text{O}_2^{\bullet-}$. The electrochemical reaction mechanisms of the generation of HO^\bullet and H_2O_2 by reduction of dissolved oxygen in the cathodic compartment was proved previously [43]. In the initial 60 min, it was believed that the non-chlorinated intermediates were not be further oxidized to CO_2 and H_2O in the cathodic compartment, which did not produce H_2O_2 by the electro-reduction of dissolved oxygen during feeding hydrogen gas. After 60 min, it was obviously that Pd/C catalyst in Pd/C gas-diffusion electrode system accelerated the two-electron reduction of O_2 to H_2O_2 when feeding air, which was consistent with CV conclusions (see Fig. 5).

As shown in Fig. 9, the mineralization degree of chlorinated organic compounds and TOC removal in the cathodic compartment showed better effects than that in the anodic compartment. In the anodic compartment of the diaphragm cell, the mechanism of the electrochemical oxidation of organics at the metallic oxide $\text{TiO}_2/\text{IrO}_2/\text{RuO}_2$ anode was very complex and not yet fully understood. It seemed that two oxidation pathways were involved in direct anodic electrochemical oxidation process by $\text{MO}_x(\text{OH}^\bullet)$ or MO_{x+1} produced on the anode surface. In the presence of oxidizable organic compounds (R), $\text{MO}_x(\text{OH}^\bullet)$ radicals should predominantly cause their complete degradation to carbon dioxide and water (electrochemical cold combustion pathway). And MO_{x+1} was supposed to react with R to generate medium oxidation products via heterogeneous catalytic oxidation at the active sites of the electrodes (chemical oxidation pathway). The degradation of aromatic compounds in the anodic compartment was supposed to be oxidized by $\text{MO}_x(\text{OH}^\bullet)$ or MO_{x+1} produced on the anode surface [44]. But for anodic oxidation, it was difficult to achieve total mineralization because of low $\text{MO}_x(\text{OH}^\bullet)$ or MO_{x+1} concentration on the anode. However, the oxidizing power of H_2O_2 , HO^\bullet and $\text{O}_2^{\bullet-}$ existed in the catholyte during O_2 -electroreduction on the Pd/C gas-diffusion cathode were very strong, which can oxidize organics to smaller molecule intermediates or to CO_2 and H_2O . Therefore, the mineralization of chlorinated organics in the cathodic compartment was better than that in the anodic compartment.

4. Conclusions

A new Pd/C gas-diffusion cathode was prepared and investigated to electrocatalytic degrade three chlorinated phenols (4-CP, 2,4-DCP, and PCP) in aqueous solutions. The electrolysis system from 15% mass fraction nitric acid pretreated activated carbon showed better electrocatalytic activity compared to those from other mass fractions nitric acid, due to the active organic function groups increased on the surface of the activated carbon. When

the ratio of Pd/C was low, Pd particles with an average size of 3.5 nm were highly dispersed in the activated carbon with an amorphous structure. In the Pd/C gas-diffusion electrode system feeding firstly with hydrogen gas and then with air, the removal efficiency for chlorinated phenols reached almost 100%, conforming to the sequence of 4-CP, 2,4-DCP and PCP, which suggested that with the increase of the number of chlorine atoms in the aromatic ring, the chloride organic compounds became more difficult to be oxidized. The Pd/C gas-diffusion cathode cannot only reductively dechlorinate chlorinated phenols by feeding hydrogen gas, but also accelerate the two-electron reduction of O_2 to H_2O_2 by feeding air. For H_2O_2 and HO^\bullet existed in the catholyte and reduction dechlorination at the cathode, the mineralization of organic compounds in the cathodic compartment was better than that in the anodic compartment. The degradation of organics was supposed to be cooperative oxidation by direct or indirect electrochemical oxidation at the anode and H_2O_2 , HO^\bullet produced by oxygen reduction at the cathode. The combined process of reduction and oxidation was in favor of improving chlorinated phenols degradation efficiency.

Acknowledgements

This work was supported by the Fundamental Research Funds for the Central Universities (no. HJ2010-6 and YX2010-32), the National Natural Science Foundation of China (Grant 20903012), Program for New Century Excellent Talents in University (no. NCET-10-0233) and Beijing Natural Science Foundation (no. 8122031), which are greatly acknowledged.

References

- [1] H.Y. Zhou, J. Han, S.A. Baig, X.H. Xu, *Journal of Hazardous Materials* 198 (2011) 7–12.
- [2] R. Navon, S. Eldad, K. Mackenzie, F.D. Kopinke, *Applied Catalysis B: Environmental* 119–120 (2012) 241–247.
- [3] C.C. Konstantinos, L. Maria, D. Yianni, *Applied Catalysis B: Environmental* 95 (2010) 297–302.
- [4] A.B. Mohamed, A.M. Sawsan, F.M. Mohamed, M.A.S. Ahmad, *Applied Catalysis B: Environmental* 107 (2011) 316–326.
- [5] M. Gomez, M.D. Murcia, J.L. Gomez, E. Gomez, M.F. Maximo, A. Garcia, *Applied Catalysis B: Environmental* 117–118 (2012) 194–203.
- [6] S. Yamazaki, Y. Fujiwara, S. Yabuno, K. Adachi, K. Honda, *Applied Catalysis B: Environmental* 121–122 (2012) 148–153.
- [7] Ch. Comninellis, *Electrochimica Acta* 39 (1994) 1857–1862.
- [8] Y.Y. Chu, W.J. Wang, M. Wang, *Journal of Hazardous Materials* 180 (2010) 247–252.
- [9] J.E. Vitt, D.C. Johnson, *Journal of the Electrochemical Society* 139 (1992) 774–780.
- [10] T. Harrington, D. Pletcher, *Journal of the Electrochemical Society* 146 (1999) 2983–2989.
- [11] L.C. Almeida, S.G. Segura, N. Bocchi, E. Brillas, *Applied Catalysis B: Environmental* 103 (2011) 21–30.
- [12] Y.Y. Chu, Y. Qian, W.J. Wang, X.L. Deng, *Journal of Hazardous Materials* 199–200 (2012) 179–185.
- [13] E. Brillas, E. Mur, J. Casado, *Journal of the Electrochemical Society* 143 (1996) L49–L53.
- [14] S. Randazzo, O. Scialdone, E. Brillas, *Journal of Hazardous Materials* 193 (2011) 1555–1564.
- [15] S. Murugesan, K. Myers, V.R. Subramanian, *Applied Catalysis B: Environmental* 103 (2011) 266–274.
- [16] J.S. Do, C.P. Chen, *Journal of Applied Electrochemistry* 24 (1994) 936–942.
- [17] K.B. Lee, M.B. Gu, S.H. Moon, *Water Research* 37 (2003) 983–992.
- [18] Y.R. Wang, W. Chu, *Water Research* 45 (2011) 3883–3889.
- [19] M.A. Oturan, M.C. Edelhah, N. Oturan, K.E. Kacemi, J.J. Aaron, *Applied Catalysis B: Environmental* 97 (2010) 82–89.
- [20] A. Kaidar, N. Sylvie, D.H. Eric, L. Jérôme, S.A. Isabelle, B. Alain, C. Michel, *Applied Catalysis B: Environmental* 104 (2011) 169–176.
- [21] E.I. Chávez, C. Arias, P.L. Cabot, F. Centellas, R.M. Rodríguez, J.A. Garrido, E. Brillas, *Applied Catalysis B: Environmental* 96 (2010) 361–369.
- [22] C.P. Leon, D. Pletcher, *Journal of Applied Electrochemistry* 25 (1995) 307–314.
- [23] A.A. Gallegos, D. Pletcher, *Electrochimica Acta* 44 (1999) 2483–2492.
- [24] A. Hirvonen, M. Trapido, J. Hentunen, J. Tarhanen, *Chemosphere* 41 (2000) 1211–1218.
- [25] P. Dabo, A. Cyr, F. Laplante, F. Jean, H. Menard, J. Lessard, *Environmental Science and Technology* 34 (2000) 1265–1268.
- [26] C.Y. Cui, X. Quan, H.T. Yu, Y.H. Han, *Applied Catalysis B: Environmental* 80 (2008) 122–128.
- [27] H. Wang, J.L. Wang, *Applied Catalysis B: Environmental* 89 (2009) 111–117.
- [28] J.P. Ramirez, J.M.G. Cortes, F. Kapteijn, M.J.I. Gomez, A. Ribera, C.S. Martinez, *Applied Catalysis B: Environmental* 25 (2000) 191–203.
- [29] M. Santiago, F. Stuber, A. Fortuny, A. Fabregat, J. Font, *Carbon* 43 (2005) 2134–2145.
- [30] S.V. Vassilev, C.B. Danheux, R. Moliner, I. Suelves, M.J. Lazaro, T. Thiemann, *Fuel* 81 (2002) 1281–1296.
- [31] Y.Y. Xue, G.Z. Lu, Y. Guo, Y.L. Guo, Y.Q. Wang, Z.G. Zhang, *Applied Catalysis A: General* 79 (2008) 262–269.
- [32] L.D.R. André, S.A. Péricles, A.G.A. Donato, S. Martin, *Applied Catalysis A: General* 277 (2004) 71–81.
- [33] T. Garcia, R. Murillo, D. Cazorla-Amoros, A.M. Mastral, A. Linares-Solano, *Carbon* 42 (2004) 1683.
- [34] H.P. Boehm, *Carbon* 40 (2002) 145–149.
- [35] H. Wang, J.L. Wang, *Applied Catalysis B: Environmental* 77 (2007) 58–65.
- [36] J.L. Figueiredo, M.F.R. Pereira, M.M.A. Freitas, J.J.M. Orfao, *Carbon* 37 (1999) 1379–1389.
- [37] Z.H. Zhu, S. Wang, G.Q. Lu, D.K. Zhang, *Catalysis Today* 53 (1999) 669–681.
- [38] J.D. Rodgers, W. Jedral, N.J. Bunce, *Environmental Science and Technology* 33 (1999) 1453–1457.
- [39] A.I. Tsyganok, I. Yamanaka, K. Otsuka, *Chemosphere* 39 (1999) 1819–1831.
- [40] Y. Yasman, V. Bulatov, I. Rabin, M. Binetti, I. Schechter, *Ultrasonics Sonochemistry* 13 (2006) 271–277.
- [41] B. Boye, M.M. Dieng, E. Brillas, *Environmental Science and Technology* 36 (2002) 3030–3035.
- [42] I.F. Cheng, Q. Fernando, N. Korte, *Environmental Science and Technology* 31 (1997) 1074–1078.
- [43] X.J. Yu, H. Wang, D.Z. Sun, L. Wu, L.W. Song, *Journal of Environmental Sciences-China* 18 (2006) 33–39.
- [44] I. Sirés, J.A. Garrido, R.M. Rodríguez, E. Brillas, N. Oturan, M.A. Oturan, *Applied Catalysis B: Environmental* 72 (2007) 382–394.